

Measuring Gaugino Soft Phases and the LSP Mass At Fermilab

S. Mrenna,^{*}

Physics Department, University of California at Davis, Davis, CA 95616, USA

G.L. Kane[†] and Lian-Tao Wang[‡]

Randall Laboratory, Dept. of Physics, Ann Arbor, MI 48109, USA

(October 14, 2018)

Abstract

Once superpartners are discovered at colliders, the next challenge will be to determine the parameters of the supersymmetric Lagrangian. We illustrate how the relative phases of the gluino, $SU(2)$, and $U(1)$ gauginos and the Higgsino mass parameter μ can be measured at a hadron collider without ad hoc assumptions about the underlying physics, focusing on Fermilab. We also discuss how the gluino and LSP masses can be measured.

^{*}mrenna@physics.ucdavis.edu

[†]gkane@umich.edu

[‡]liantaow@umich.edu

I. INTRODUCTION

Presently there is considerable indirect evidence that the Standard Model (SM) is extended to a supersymmetric SM (SSM), and that at least some superpartners are light enough to be produced at the LEP or Fermilab colliders. There is some motivation that gluinos are light and will be produced copiously at Fermilab in the next run [1], based on the success of supersymmetry in explaining electroweak symmetry breaking, which relates superpartner masses to the Z boson mass. Once superpartners are discovered, the next step will be to measure the parameters of the Lagrangian, and then to learn the underlying theory that leads to such a Lagrangian (technically, the softly broken supersymmetric Lagrangian).

Before using existing information to constrain the Lagrangian, the minimal case has over 100 free parameters [2], of which at most two are directly measurable, the gluino and gravitino masses, since these are the only ones that do not mix to form mass eigenstates. The parameters consist of (at least) 33 masses, 40 phases, and 32 super-CKM type angles relating flavor and mass eigenstates. The phases can all induce CP violating effects, and it has recently been argued that all CP violation could be explained by these SUSY soft phases [3]. The phases affect much more than CP violating observables – cross sections, branching fractions, radiative corrections, the LSP relic density, LEP Higgs boson limits, etc. [4–6]. In general, superpartner production cross sections, decay rates and kinematic distributions depend on the phases, as we illustrate in this paper. The same gluino phase ϕ_3 that we consider is also measurable in CP violation in the Kaon system [3].

In the past [7], it was argued that the supersymmetric soft phases must be small because they would otherwise induce neutron and electron electric dipole moments larger than the experimental upper limits. However, recently it has been shown [8–10] that large phases are not disallowed by current data provided that reasonable relations exist among them. In fact, one expects relations among parameters in typical theories. For example, a model produced by embedding the MSSM on a particular configuration of D-branes naturally has large phases and small EDMs [11]. The phases of the supersymmetry Lagrangian may or may not be small – it will be necessary to measure them to find out.

In this paper we illustrate how the presence of phases affect observables and can be measured in gluino production and decay. The gluino production cross section does not depend on the phases, but the gluino decay does. To understand the essence of what happens, we consider the tree level production of gluino pairs followed by the decay $\tilde{g} \rightarrow q\bar{q}\tilde{N}_1$, where \tilde{N}_1 is the lightest neutralino and the LSP. The generalization to other production and decay channels is straightforward but complicated. For simplicity, we assume that squarks are significantly heavier than gluinos, so that squarks decouple from the production cross section.

The phases of interest enter initially in the gaugino and higgsino mass parameters $M_3 e^{i\phi_3}$,

$M_2 e^{i\phi_2}$, $M_1 e^{i\phi_1}$, and $\mu e^{i\phi_\mu}$ in the Lagrangian. For our example, the gluino phase enters directly, and the others through the neutralino mass matrix

$$\mathbf{Y} = \begin{pmatrix} M_1 e^{i\phi_1} & 0 & -M_Z s_\beta s_W & M_Z c_\beta s_W \\ 0 & M_2 e^{i\phi_2} & M_Z c_\beta c_W & -M_Z c_\beta c_W \\ -M_Z s_\beta s_W & M_Z s_\beta c_W & 0 & -\mu e^{i\phi_\mu} \\ M_Z c_\beta s_W & -M_Z c_\beta c_W & -\mu e^{i\phi_\mu} & 0 \end{pmatrix}, \quad (1.1)$$

where our notation is $s_\beta = \sin \beta$, $c_\beta = \cos \beta$, $s_W = \sin \theta_W$ and $c_W = \cos \theta_W$. This matrix can be diagonalized by a 4×4 unitary matrix \mathbf{N} , i.e. $\mathbf{Y}_D = \mathbf{N}^\dagger \mathbf{Y} \mathbf{N}$. $U(1)$ symmetries of the Lagrangian allow reparameterizations [2,9,13], so that only the combinations $\phi_3 - \phi_2$, $\phi_3 - \phi_1$, and $\phi_3 + \phi_\mu$ are invariant and, thus, observable.

For the case considered here, we will see that only one phase can be measured, ϕ_{eff} , which depends on all of these Lagrangian phases (and also on $\tan \beta$ and masses). When additional decay channels are included, different combinations of the Lagrangian phases can be measured. Measurements at Fermilab alone could establish that ϕ_{eff} was non-zero, and therefore that at least one phase was non-zero. That would mean that at least one phase was fairly large in order to give a significant numerical effect. It is more difficult to show that the phases are small, since some combinations of them may be small but not others. A combination of measurements from electric dipole moments, b -factories, and high energy colliders producing superpartners would establish that the phases were small if they indeed were.

It is important to emphasize that we are following a general procedure, with no model dependent assumptions about phases being small or related to one another, or masses being degenerate, etc. Our simplifying assumptions are used only to present the results simply; the procedure can be followed without simplifying assumptions once real data once is available.

In addition to phases, two quantities are particularly important to measure because they affect many other results. One is the LSP mass. The LSP is a very good candidate for the cold dark matter of the universe. If superpartner events are observed with an escaping LSP it will, of course, greatly encourage us to indeed believe the LSP is the CDM. But that is not established until a calculation of the relic density is carried out that shows $\Omega_{LSP} \sim 1/4$, and the calculation cannot be done [12] until the LSP mass and couplings are measured and perhaps some superpartner masses. If the LSP candidate interactions are observed in explicit dark matter detection experiments, the LSP mass deduced from those can be compared to the LSP collider mass. In order to measure the LSP mass we provide a two step procedure.

The second important quantity is $\tan \beta$, but it is very difficult to measure. Here, it occurs in the \tilde{N}_1 couplings (see next section) to quark-antiquark pairs, which enter into ϕ_{eff} along with phases and masses. To the best of our knowledge, $\tan \beta$ can only be definitively

measured at a lepton collider with a polarized beam and sufficient energy to produce some superpartners [4].

In the next section we explain the formalism and derive the relevant distributions.

II. RELEVANT LAGRANGIAN AND ANALYTICAL RESULTS

The general gluino mass term in the MSSM Lagrangian is

$$\mathcal{L} \supset -\frac{1}{2}(M_3 e^{i\phi_3} \lambda_g \lambda_g + M_3 e^{-i\phi_3} \bar{\lambda}_g \bar{\lambda}_g), \quad (2.1)$$

where λ_g is a Majorana spinor. With the field redefinition $\psi_g = G \lambda_g$, $G \equiv e^{i\frac{\phi_3}{2}}$, the kinematic mass of the gluino is real. After this redefinition, the quark-squark-gluino vertex is

$$\mathcal{L}_{q\bar{q}\tilde{g}} = -g_s \sqrt{2} T_{jk}^a (G^* \bar{g}_a P_L q_i^k \tilde{q}_{iL}^{j*} - G^* \bar{g}_a P_R q_i^k \tilde{q}_{iR}^{j*} + G \bar{q}_i^j P_L \tilde{g}_a \tilde{q}_{iL}^{j*} - G \bar{q}_i^j P_R \tilde{g}_a \tilde{q}_{iR}^{j*}), \quad (2.2)$$

where the lower index i is the flavor label, and the upper indices j and k label the color of (s)quarks.

The quark-antiquark-neutralino vertex is

$$\mathcal{L}_{q\bar{q}\tilde{N}_1} = -g\sqrt{2} f_i^L \bar{q}_i P_R \tilde{N}_1 \tilde{q}_{iL}^j + g\sqrt{2} f_i^{R*} \bar{q}_i P_L \tilde{N}_1 \tilde{q}_{iR}^j + h.c., \quad (2.3)$$

where

$$f_i^L = T_{3i} N_{12} - \tan \theta_W (T_{3i} - e_i) N_{11} \quad f_i^R = \tan \theta_W e_i N_{11}. \quad (2.4)$$

The N_{ij} are the complex elements of the unitary matrix which diagonalizes the neutralino mass matrix, and depend on the phases ϕ_1, ϕ_2, ϕ_μ .

The production of gluino pairs does not depend upon the phases, and can be calculated using the standard CP-conserving Feynman rules of the MSSM [14]. In the limit that the squark masses are very heavy, the spin structure is analogous to that of top quark pair production [16]. The details of this calculation are contained in the appendix. We have included this spin structure in our calculation to test whether it influences any physical observable. In the end, we observed no spin correlations, so the calculation is only mildly interesting.

Apart from an overall color factor, the polarized decay amplitude squared for a gluino with spin vector s is:

$$\begin{aligned} |\tilde{g}(s) \rightarrow q_i \bar{q}_j N_1|^2 = & |0|_L^2 + 2\delta_L \left\{ m_{\tilde{g}} (|\alpha_L|^2 p_1 \cdot p_j s \cdot p_i - |\beta_L|^2 p_1 \cdot p_i s \cdot p_j) \right. \\ & + 2m_1 \text{Re}(\alpha_L \beta_L^*) (p_g \cdot p_j s \cdot p_i - p_g \cdot p_i s \cdot p_j) \\ & \left. - 2m_1 \text{Im}(\alpha_L \beta_L^*) \epsilon^{\mu\nu\rho\sigma} p_{g\mu} s_\nu p_{i\rho} p_{j\sigma} \right\} + (L \rightarrow R). \end{aligned} \quad (2.5)$$

The spin independent piece $|0|^2 = |0|_L^2 + |0|_R^2$ is

$$\frac{1}{2} \left(|\alpha_L|^2 (\bar{t} - m_1^2)(m_g^2 - \bar{t}) + |\beta_L|^2 (\bar{u} - m_1^2)(m_g^2 - \bar{u}) + 2\text{Re}(\alpha_L \beta_L^*) m_1 m_{\bar{g}} \bar{s} \right) + (L \rightarrow R), \quad (2.6)$$

with the couplings

$$\begin{aligned} \alpha_L &= 2g_s g G f_i^{L*} / M_L^2 & \alpha_R &= 2g_s g G^* f_i^R / M_R^2 \\ \delta_L &= 1, \delta_R = -1 & \beta_L &= \alpha_L^* & \beta_R &= \alpha_R^*, \end{aligned} \quad (2.7)$$

and the kinematic variables $\bar{s} = (p_i + p_j)^2$, $\bar{t} = (p_g - p_j)^2$, and $\bar{u} = (p_g - p_i)^2$. The gluino and neutralino four-momenta are denoted by p_g and p_1 , respectively, with $p_g^2 = m_g^2$ and $p_1^2 = m_1^2$. p_i and p_j denote the quark and antiquark four-momenta, and we assume $p_i^2 = p_j^2 = 0$. These expressions have been summed over the spins of the final state particles. In the limit that the phases are zero, these expressions reproduce the standard results. A similar formulae was derived earlier for the three-body decay of a heavy neutralino into a lepton-antilepton pair and a lighter neutralino [6]. In writing out the expressions (2.7), we have assumed universality of the squark masses (except for the top squarks, which are not important for the analysis considered here)

$$m_{\tilde{q}_{iL}} = M_L, m_{\tilde{q}_{iR}} = M_R,$$

where index i runs through five flavors of squarks, and that the squark masses are much larger than any momentum q^2 exchanged in the decay, making the replacement

$$(q^2 - M^2)^{-1} \rightarrow -M^{-2}.$$

Our methodology is valid regardless of this assumption, and it is not necessary for analyzing the real data. To generalize these expressions, one would simply replace $M_{L,R}^2$ by $M_{L,R}^2 - \bar{t}$ in $\alpha_{L,R}$ or by $M_{L,R}^2 - \bar{u}$ in $\beta_{L,R}$.

Eq. (2.6) can be simplified, using the fact that $|\alpha_L| = |\beta_L|$ and $|\alpha_R| = |\beta_R|$ (which is only true with our simplifications), to

$$\frac{1}{2} (|\alpha_L|^2 + |\alpha_R|^2) \left[(\bar{t} - m_1^2)(m_g^2 - \bar{t}) + (\bar{u} - m_1^2)(m_g^2 - \bar{u}) + 4 \cos \phi_{\text{eff}} m_1 m_{\bar{g}} \bar{s} \right]. \quad (2.8)$$

The effective phase ϕ_{eff} is defined by

$$\cos \phi_{\text{eff}} = \frac{|\alpha_L|^2 \cos \phi_L + |\alpha_R|^2 \cos \phi_R}{|\alpha_L|^2 + |\alpha_R|^2} \quad (2.9)$$

where ϕ_L is $\arg(\alpha_L)$ and ϕ_R is $\arg(\alpha_R)$. There is a summation over the index i , which specifies the quantum numbers of each squark flavor.

The expressions for the production of gluino pairs and the decay outlined above are the starting point for our phenomenological analysis. Focusing on the decays, we note that the effect of phases appears in Eq. (2.8) as the coefficient of the quark–antiquark invariant mass. Therefore, we expect to observe sensitivity to phases in that distribution. A similar observation was made for the case of three-body decays of neutralinos [6]. The form of Eq. (2.9) guarantees that phase effects will not decouple if one of the squarks is much heavier than the other. We need not have $M_R \sim M_L$ to obtain a sizable effect.

Although most generally there should be four relevant phases, by suitable field redefinition, it can be shown that only combinations $\phi_1 - \phi_3$, $\phi_2 - \phi_3$ and $\phi_3 + \phi_\mu$ are relevant for this process. In fact, these are all R-invariant physical observables [2,9,13], and therefore cannot be further rotated away by field redefinition.

Finally, the phases are a manifestation of CP-violation, and their presence should be manifest in a CP-violating observable. One example considered here is the contraction of particle four-momenta with the 4-dimensional Levi-Cevita tensor.

III. PHENOMENOLOGY AND MEASURING PARAMETERS

We concentrate on the signature of 4 jet plus missing transverse energy \cancel{E}_T which is naturally expected for the process considered here. To define the signal, we specify the following cuts, motivated by the DØ Run I multijet and \cancel{E}_T analysis [18]:

$$\begin{aligned} \cancel{E}_T > 75 \text{ GeV}, \mathcal{H}_T > 100 \text{ GeV}, |\eta^{\text{jet}}| < 2.5, p_T^{\text{jet}} > 15 \text{ GeV}, \Delta R_{ij} > 0.5, \\ 0.1 < \Delta\phi_{\text{jet}, \cancel{E}_T} < \pi - 0.1, \sqrt{(\pi - \Delta\phi_{1, \cancel{E}_T})^2 + \Delta\phi_{2, \cancel{E}_T}^2} > 0.5 \end{aligned} \quad (3.1)$$

where ΔR_{ij} is the $\eta - \phi$ separation of jets i and j , \mathcal{H}_T is the scalar sum of p_T^{jet} excluding the leading jet in E_T , and 1 and 2 are subscripts denoting the leading and next-to-leading jet in E_T . The $\Delta\phi$ cuts are necessary to reduce the fake \cancel{E}_T backgrounds that arise when part of a jet is lost. For this analysis, we ignore the fact that some background events will pass these cuts. Their effect can only be subtracted statistically, and they will degrade the results presented here. The application of cuts biases the final event sample, and the details of the proposed measurements presented here will depend upon them. The exact cuts needed to reduce backgrounds (primarily the cut on \cancel{E}_T) will not be known until the experiments begin to collect data at high luminosity. These cuts are meant to be representative of what will actually be done. Finally, we smear jet energies by a Gaussian resolution ($\sigma_E = .80\sqrt{E}$, E measured in GeV) typical of Tevatron experiments.

Some of the measurements will benefit if the flavor of the jets can be tagged. If all of the jets originate from light quarks, then there is a threefold ambiguity in assigning pairs of daughter jets to a mother gluino. We have tested various kinematic quantities, and find

that choosing the combination which minimizes the sum of the square of the jet pair masses does fairly well in picking the correct one. However, there *is* a substantial degradation in the measurements with this choice. On the other hand, if two of the jets are b -tagged, then the ambiguity is substantially reduced. We estimate that this can retain roughly a fraction of $2 \times .2 \times .8 \times .36 = .12$ of all events, where .36 is an estimate of the double b -tag efficiency. Charm quark tagging is also possible. Of course, heavy flavor decays have to be corrected for the energy lost to neutrinos, an effect which we do not simulate here. Finally, jet charge can be measured for even light quarks, using the fact that a u -quark will fragment to a leading π^0, π^+, K^+ with (very) roughly the same probability, while a \bar{d} -quark will fragment to a leading π^+, π^0, K^0 . Therefore, if four jets are observed with leading tracks of charge $+, -, 0$ and 0 , the combinations $(+, -)$ and $(0, 0)$ would be preferred.

As explained earlier, we have made the simplification that the squark masses are universal and heavy in order to present the results simply. Since the mass splitting $\Delta M_{\tilde{g}\tilde{N}_1} \equiv m_{\tilde{g}} - m_{\tilde{N}_1}$ can be measured in a straightforward manner, we choose the value 145 GeV for our numerical work, and consider gluino masses from 200 to 350 GeV in steps of 25 GeV. The final results will not depend dramatically on the value of the mass splitting, provided that it is large enough so that jets from the gluino decay are measurable.

A. Coupling Measurements

Even with the simplifications made in this analysis, the gluino decay distribution depends on several parameters of the MSSM Lagrangian. From Eq. (2.8), it is clear that we are sensitive to only an overall normalization and the relative strength of the \bar{s} term to \bar{t} and \bar{u} . We can perhaps measure the overall normalization through the effect of the decay width on the shape of the gluino invariant mass distribution, but the width is much smaller than the typical energy resolution. The branching ratio for the $q\bar{q}\tilde{N}_1$ decay may be inferred from the number of events observed, but one would have to measure other decay modes to make use of this information. Therefore, we concentrate on methods to determine ϕ_{eff} .

One method is illustrated in Figs. 1 and 2. In Fig. 1, we plot the invariant mass distribution of the jets assuming that the jet pairs can be unambiguously identified with a particular gluino. This would require, for example, that two jets have a heavy flavor tag and two jets have an anti-tag. The three curves (solid, long-dash, short-dash) show the effect of $\phi_{\text{eff}} = 0, \pi/2, \pi$. From $\phi_{\text{eff}} = 0 \rightarrow \pi$, the peak has shifted by approximately 25 GeV. If limited statistics require a combination of all data, so that tagging cannot be used, the one method for pairing the jets is to minimize the sum of the squares of the invariant masses. The resultant invariant mass distribution is shown in Fig. 2. There is still a phase dependence, but the miscombination has washed the effect out somewhat (the peak has shifted roughly 10 GeV).

To estimate how well we can actually distinguish these distributions, we generated sets of fake data based on the distribution for $\phi_{\text{eff}} = \pi$ and compare them to the ideal distribution for $\phi_{\text{eff}} = 0$. The distribution of χ^2 based on this comparison gives some indication of the sensitivity of the experiments. We quote the value of χ^2 that contains 5% of the total area of the χ^2 distribution. We could also quote the median value of the distribution, but this would give no indication as to the size of the low-side tail. The interpretation of the χ^2 depends upon how the fake data was binned in a histogram. For this case, $\chi^2 = 1.9$ and 2.5 corresponds to a 95% and a 99% confidence level, respectively. Therefore, a χ^2 that is far from 2.5 indicates a good separation of the two distributions. A χ^2 near 1 means the two distributions are consistent with each other. We first consider the case when the two daughter jets can be paired correctly with the mother gluino. Assuming an efficiency of 0.2 for correctly tagging the jet pair, $m_{\tilde{g}} = 250(350)$ GeV, and 2 fb^{-1} of data, the comparison yields $\chi^2 = 11.7(1.3)$. The value $\chi^2 = 11.7$ for $m_{\tilde{g}} = 250$ GeV shows that the two distributions are quite distinct with just 2 fb^{-1} of data. On the other hand, with only 2 fb^{-1} of data, the distribution for $\phi_{\text{eff}} = \pi$ and $m_{\tilde{g}} = 350$ GeV is fairly consistent with that for $\phi_{\text{eff}} = 0$. However, with 10 fb^{-1} of data, $\chi^2 = 6.7$. Accepting miscombinations of the jet pairs, but an efficiency of 1.0, the 2 fb^{-1} numbers are $23.7(2.1)$ for $m_{\tilde{g}} = 250(350)$ GeV. With 10 fb^{-1} , the χ^2 for $m_{\tilde{g}} = 350$ GeV increases to 11.0. In all cases, we assume a branching ratio of 1.0 for the four jet decay mode. In general, we find that the increase in sensitivity scales linearly with integrated luminosity. Despite the fact that miscombination of the jet pairs distorts the invariant mass distribution, a large ϕ_{eff} dependence still remains, so that the additional statistics makes for a better separation of the two hypotheses ($\phi_{\text{eff}} = 0$ or π).

From pure kinematic considerations, the invariant mass distribution of the jet pairs has an end point at $\Delta M_{\tilde{g}\tilde{N}_1} \equiv m_{\tilde{g}} - m_1$ (the end point is smeared if we choose the wrong pairing of jets and by energy resolution). For the measurements discussed above, and others discussed below, it is important to measure the endpoint with sufficient accuracy. This requires a detailed knowledge of both the number of background events and the shape of the background distribution (as well as the same quantities for the signal). The cuts of Eq. (3.1) are somewhat more restrictive than those used in the DØRun I analysis [18], but we can use them to estimate the background at 0.5 pb . This means that the signal to background ratio for $m_{\tilde{g}} = 250$ GeV is roughly 1, decreasing to $1/10$ for $m_{\tilde{g}} = 350$ GeV. Tighter cuts may be desired to establish a signal for heavier gluino masses and to measure parameters. For two very different choices of the background shape, and for $\cos \phi_{\text{eff}} \simeq 1$ and $m_{\tilde{g}} = 250$ GeV, the endpoint of the invariant mass distribution can be measured to a few GeV. There is a systematic shift in the fit endpoint and roughly twice error for when $\cos \phi_{\text{eff}} \simeq -1$, but this is an artifact of approximating the mass spectrum by a straight line near the endpoint. This will not occur in a real analysis that includes the full shape of the signal distribution. While

the full invariant mass distribution, including miscombinations, gave a better separation of different parameters, a tagged sample of events will probably yield a cleaner measurement of the endpoint of the invariant mass distribution.

One distribution that does not depend on the jet pairing or the measurement of the endpoint is based on contracting the jet 4-momenta with the Levi-Cevita tensor. We define:

$$\epsilon = \frac{\epsilon_{\mu\nu\rho\sigma} p_1^\mu p_2^\nu p_3^\rho p_4^\sigma}{E_1 E_2 E_3 E_4}, \quad (3.2)$$

where the momentum components are measured in the laboratory frame. This distribution is shown in Fig. 3. The distinguishing feature is the half width at half maximum for the curves, which varies from 1.0 to 1.5 as $\phi_{\text{eff}} = 0 \rightarrow \pi$ (this is for the case of $m_{\tilde{g}} = 250$ GeV, but the variation for other masses is small). We estimate the sensitivity as for the invariant mass distribution. For $m_{\tilde{g}} = 250$ GeV, $\chi^2 = 9.3$ with only 2 fb^{-1} , while for $m_{\tilde{g}} = 350$ GeV, $\chi^2 = 1.0(4.8)$ for $2 (10) \text{ fb}^{-1}$. Therefore, the untagged jet-jet invariant mass distribution yields a superior separation of $\phi_{\text{eff}} = 0$ or π compared to any other method considered here. The best result will come from combining several observables.

For Figs. 1-3, we have used the particular example of $m_{\tilde{g}} = 250$ GeV. The invariant mass and ϵ distributions discussed above are not very sensitive to this number, so the existence of CP-violating phases can be established without knowing the masses in the problem (the mass splitting is inferred from the endpoint of invariant mass distribution). In the next subsection, however, we will demonstrate that the masses can also be known.

B. Mass Measurements

From the observed mass splitting $\Delta M_{\tilde{g}\tilde{N}_1}$, a measurement of $m_{\tilde{g}}$ will accordingly give us a measurement of m_1 . Even in the case when the mother gluino is not tagged, comparison of different m_{ij} distributions can yield a measurement of $\Delta M_{\tilde{g}\tilde{N}_1}$. This is demonstrated in Figs. 1 and 2 previously mentioned.

By comparing the total number of events to the theoretical prediction for the cross section, one can estimate $m_{\tilde{g}}$, and therefore determine all the masses in the problem. However, the total number of events really only measures $\sigma \times BR^2(\tilde{g} \rightarrow q\bar{q}\tilde{N}_1)$, and some decay modes may not be measurable at a hadron collider. What is preferable is a statistical measure of the gluino mass based on kinematics. As a motivation, we direct the reader to the measurements of the top quark mass in dilepton events, which can be performed even though there are two neutrinos per event [19]. Given all the kinematic constraints for $t\bar{t}$ production and decay, there is actually only one unknown, and the momenta of the neutrinos can be reconstructed (there are four solutions) for an assumed top quark mass. There is a wide range of masses m_t that yield “reasonable” solutions, but a probability can be assigned to each m_t by comparing the resultant kinematic distributions to those expected for the assumed m_t .

The case of gluino decay is more complicated, since there are no M_W constraints. Even after specifying $m_{\tilde{g}}$, the longitudinal momentum p_z of the LSP's is not fixed. We proceed by making simple fits (using our parton level generator) to p_z as a function of $m_{\tilde{g}}$ (the sum of a wide and a narrow Gaussian), properly normalized to unity. The individual p_z values are not noticeably correlated, and we assume they are independent in making the fit. For each event, a range of values for $m_{\tilde{g}}$ is assumed, and an integration is performed over the two p_z distributions (the integral is replaced by a finite sum). For each fixed value of p_z^1, p_z^2 , and $m_{\tilde{g}}$, the full kinematics (up to multiple solutions) are reconstructed. Finally, a Gaussian weight or probability is assigned to each $m_{\tilde{g}}$ based on the difference $(\sqrt{\hat{s}} - 2m_{\tilde{g}})/(20 \text{ GeV})$.

The resultant distributions as a function of $m_{\tilde{g}}$ are displayed in Fig. 4 for the correct assignment of jets to a mother gluino (this assumes picking those events which satisfy a tagging as outlined above). The same distributions using the minimum m^2 algorithm are shown in Fig. 5. First, we note that we always reconstruct the correct mass (the peak of the weight function) within about 10 GeV for the correct assignment of jets. The case of $\phi_{\text{eff}} = \pi$ seems to yield a larger mismeasurement, but this is not quite correct. For simplicity, we have used the expected p_z distribution for the case of $\phi_{\text{eff}} = 0$ in all cases. However, we showed above that the existence of a phase can be inferred independently of the gluino mass, so the correct distribution can and should be used for each phase. Secondly, the reconstructed value considering combinatoric ambiguities (Fig. 5) is always roughly 25 GeV higher than the real mass, which can be corrected. Also, the distributions are much wider, so there will be a greater uncertainty in the measured mass. To estimate how well the masses can be measured, we fit a Gaussian to the distribution for $m_{\tilde{g}} = 250 \text{ GeV}$ around the peak and recorded the error on the fit mean. Allowing for miscombinations of the jet pair, the fit mean was $272 \pm 5(2) \text{ GeV}$ for 2 (10) fb^{-1} of data. Assuming the correct jet pairing, but an efficiency of 0.2, the fit mean was $259 \pm 9(4) \text{ GeV}$ for 2 (10) fb^{-1} of data.

The method outlined here is merely a simple demonstration of principle. While details such as soft gluon radiation, non-Gaussian errors in energy measurements, and background contamination would degrade our results, it is also possible that more sophisticated pattern recognition techniques would yield a net improvement.

IV. CONCLUSION

In this paper, we have considered some of the effects of CP-violating phases from the supersymmetry Lagrangian on the phenomenology of gluino pair production and decay. Such phases also affect non-CP-violating observables. Our specific results are for the Fermilab collider, but the general approach applies equally well to the future LHC collider. We have also considered the issue of measuring sparticle masses, which is not particular to the existence of the phases. Although our analysis uses certain simplifications in order to

demonstrate analytically how the phases enter, the method we present here shows that those measurements can be done if we have experimental data for that process. Our method can be used as a prototype for more complete analyses to treat real experimental data.

We concentrated on the case of gluino pair production, followed by the gluino decay to a quark–antiquark pair and a neutralino LSP. We found that there are simple measurements of the gluino decay products which are sensitive to a combination of phases and couplings which can be parametrized by an angle ϕ_{eff} . If ϕ_{eff} is non-zero, then it is a sign of CP violation originating in the supersymmetry soft–breaking Lagrangian.

We have also demonstrated a method to measure the LSP mass. This is based on first measuring the gluino mass $m_{\tilde{g}}$, even though there are two invisible LSP’s in each event. The method is similar to that used to measure the top quark mass in dilepton events: by comparing the observed kinematics of an event to the theoretical prediction for a range of assumed gluino masses, one can determine which gluino mass is most consistent with the data. In our analysis, the most consistent gluino mass is very close to the real gluino mass used to generate events. Then, once $m_{\tilde{g}}$ is known, the LSP mass is determined from the endpoint of the jet–jet invariant mass. The measured gluino and LSP mass are not the exact quantities that appear in the MSSM Lagrangian. The physical gluino mass $m_{\tilde{g}}$ can be related to the gluino mass parameter M_3 through QCD, but this does require some knowledge of the squark masses. More measurements will be needed to relate m_1 to the parameters M_1 , M_2 , μ , and $\tan\beta$.

If Supersymmetry is responsible for stabilizing the hierarchy between the weak and Planck scales, then there is a strong possibility that sparticles will be produced in the near future at the Tevatron. If the gluino is light enough, it will be produced in quantity, allowing its discovery and, as argued in this paper, a measurement of its and other sparticle properties. Based on our present knowledge, these measurements might indicate that Supersymmetry is responsible for all of CP-violation and/or that a neutralino LSP constitutes the dark matter of the universe.

ACKNOWLEDGEMENTS

We thank M. Brhlik, L. Everett, G. Grim, R. Breedon, and J.D. Wells for useful comments and criticisms.

APPENDIX: CALCULATION OF PRODUCTION RATES

To maximize the sensitivity to couplings, we calculated the tree level gluino pair production processes including the spin correlations. We followed closely the calculations of $t\bar{t}$ production in the “off-diagonal basis” [15–17]. When the squark masses are heavy, one finds

the same topology of Feynman diagrams for the $q\bar{q} \rightarrow \tilde{g}\tilde{g}$ subprocess as for $t\bar{t}$ production, and the latter results can be used directly with a simple modification of the color factor. The relevant expressions can be found in the above references. To summarize, in the off-diagonal basis, when the gluinos are produced in the narrow width approximation, only the spin combinations (\uparrow, \downarrow) or (\downarrow, \uparrow) occur, where the gluino spin is quantized along the special axis that defines the basis (in the rest frame of the gluino, the spin vector makes an angle $\pi - \xi$ with respect to the gluino direction of motion in the gluino pair rest frame; The angle ξ is related to the scattering angle θ^* in the gluino pair rest frame and the gluino velocity via the relation $\tan \xi = \sqrt{1 - \beta^2} \tan \theta^*$). Once the gluino decay is included, there can be interference between the (\uparrow, \downarrow) and (\downarrow, \uparrow) amplitudes, but these are suppressed by a factor of β^2 . To simplify our phenomenological analysis, we ignored this interference effect. This approximation was justified in the end, since we observed no spin correlations between the two gluino decays. Each gluino was decayed with a distribution given by the formulae of Sec. II.

The subprocess $gg \rightarrow \tilde{g}\tilde{g}$ has a more complicated spin structure, and is numerically less important than the $q\bar{q}$ subprocess at the Tevatron for the masses considered here. For completeness, we included this subprocess in our final results. The structure is almost identical to that for $gg \rightarrow t\bar{t}$, except for the overall color factor and the replacement $(9 + 7 \cos^2 \theta^*) \rightarrow (3 + \cos^2 \theta^*)$ in the formulae of Ref. [17]. We included the different contributions from (\uparrow, \uparrow) , (\downarrow, \downarrow) , (\uparrow, \downarrow) and (\downarrow, \uparrow) and added the decays ignoring the possible interference. Again, this is justified by the fact that none of our observables depended significantly on the spin correlations.

For the full calculation, we used CTEQ3M structure functions, NLO running for α_s , and evaluated structure functions and α_s at the common scale $Q = m_{\tilde{g}}$. This choice of scale reproduces well the total cross section from a complete NLO calculation [20].

While we observed no spin correlations in our final results, one may wonder how higher order QCD corrections may affect them. As observed in Ref. [21], to a very good approximation, similar NLO cross sections can be reproduced using the tree level cross section and kinematics folded with parton showering using a modified parton distribution function. Since the parton showering only boosts the gluino pair, it does not upset the spin correlations.

REFERENCES

- [1] G.L. Kane and S.F. King, Phys. Lett. **B451**, 113 (1999).
- [2] S. Dimopoulos and D. Sutter, Nucl. Phys. **B452**, 496 (1995).
- [3] M. Brhlik, L. Everett, G.L. Kane, S.F. King and O. Lebedev, hep-ph/9909480.
- [4] M. Brhlik and G.L. Kane, Phys. Lett. **B437**, 331 (1998);
- [5] T. Ibrahim and P. Nath, Phys. Lett. **B418**, 98 (1998); T. Falk, K.A. Olive and M. Srednicki, Phys. Lett. **B354**, 99 (1995); A. Pilaftsis and C.E. Wagner, Nucl. Phys. **B553**, 3 (1999); D.A. Demir, Phys. Rev. **D60**, 055006 (1999); V. Barger, T. Han, T. Li and T. Plehn, hep-ph/9907425; T. Ibrahim and P. Nath, hep-ph/9908443.
- [6] S.Y. Choi, H.S. Song and W.Y. Song, hep-ph/9907474; S.Y. Choi, hep-ph/9910325.
- [7] M. Dugan, B. Grinstein and L. Hall, Nucl. Phys. **B255**, 413 (1985).
- [8] T. Ibrahim and P. Nath, Phys. Rev. **D58**, 111301 (1998), Erratum-ibid **D60**, 099902 (1999); T. Ibrahim and P. Nath, Phys. Rev. **D57**, 478 (1998), Erratum-ibid **D58**, 019901 (1998), Erratum-ibid **D60**, 079903 (1999).
- [9] M. Brhlik, G.J. Good and G.L. Kane, Phys. Rev. **D59**, 115004 (1999).
- [10] S. Pokorski, J. Rosiek and C.A. Savoy, hep-ph/9906206.
- [11] M. Brhlik, L. Everett, G.L. Kane and J. Lykken, Phys. Rev. Lett. **83**, 2124 (1999); Ibid, hep-ph/9908326.
- [12] M. Brhlik, D. Chung, and G.L. Kane, in preparation.
- [13] S. Dimopoulos and S. Thomas, Nucl. Phys. **B465**, 23 (1996).
- [14] H.E. Haber and G.L. Kane, Phys. Rept. **117**, 75 (1985).
- [15] S. Parke and Y. Shadmi, Phys. Lett. **B387**, 199 (1996) hep-ph/9606419.
- [16] G. Mahlon and S. Parke, Phys. Rev. **D53**, 4886 (1996).
- [17] G. Mahlon and S. Parke, Phys. Lett. **B411**, 173 (1997).
- [18] S. Abachi *et al.* [D0 Collaboration], Phys. Rev. Lett. **75**, 618 (1995).
- [19] B. Abbott *et al.* [D0 Collaboration], Phys. Rev. Lett. **80**, 2063 (1998).
- [20] W. Beenakker, R. Hopker, M. Spira and P.M. Zerwas, Nucl. Phys. **B492**, 51 (1997) hep-ph/9610490.

[21] S. Mrenna, hep-ph/9902471.

FIGURES

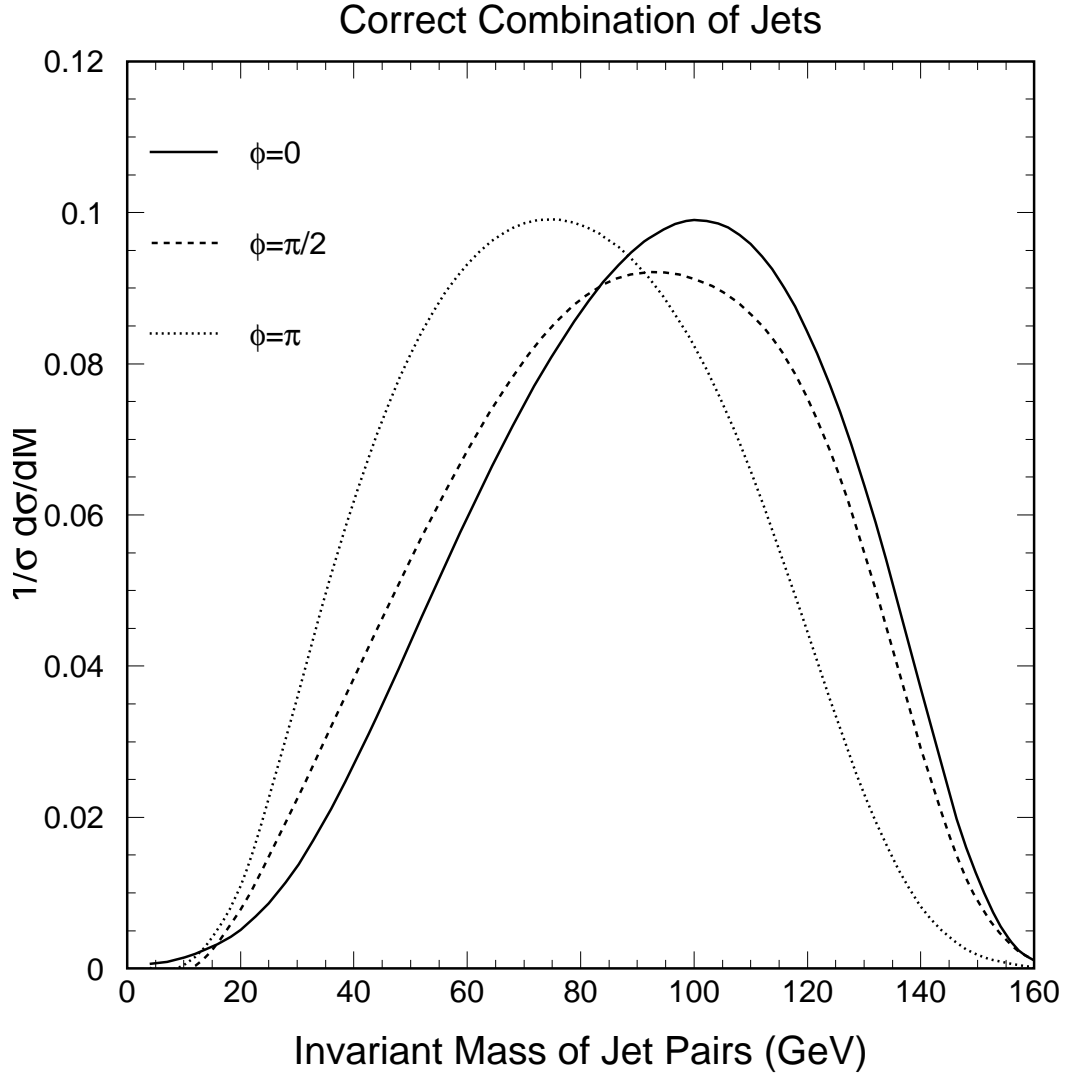


FIG. 1. The invariant mass distribution of jet pairs from gluino pair production and decay at the Tevatron. The correct combination of jet pairs is used. The distributions for three choices of the effective phase are shown. A gluino mass of 250 GeV and a mass splitting between the gluino and LSP of 145 GeV is assumed. Jet energy resolution is responsible for shifting the endpoint upwards from 145 GeV.

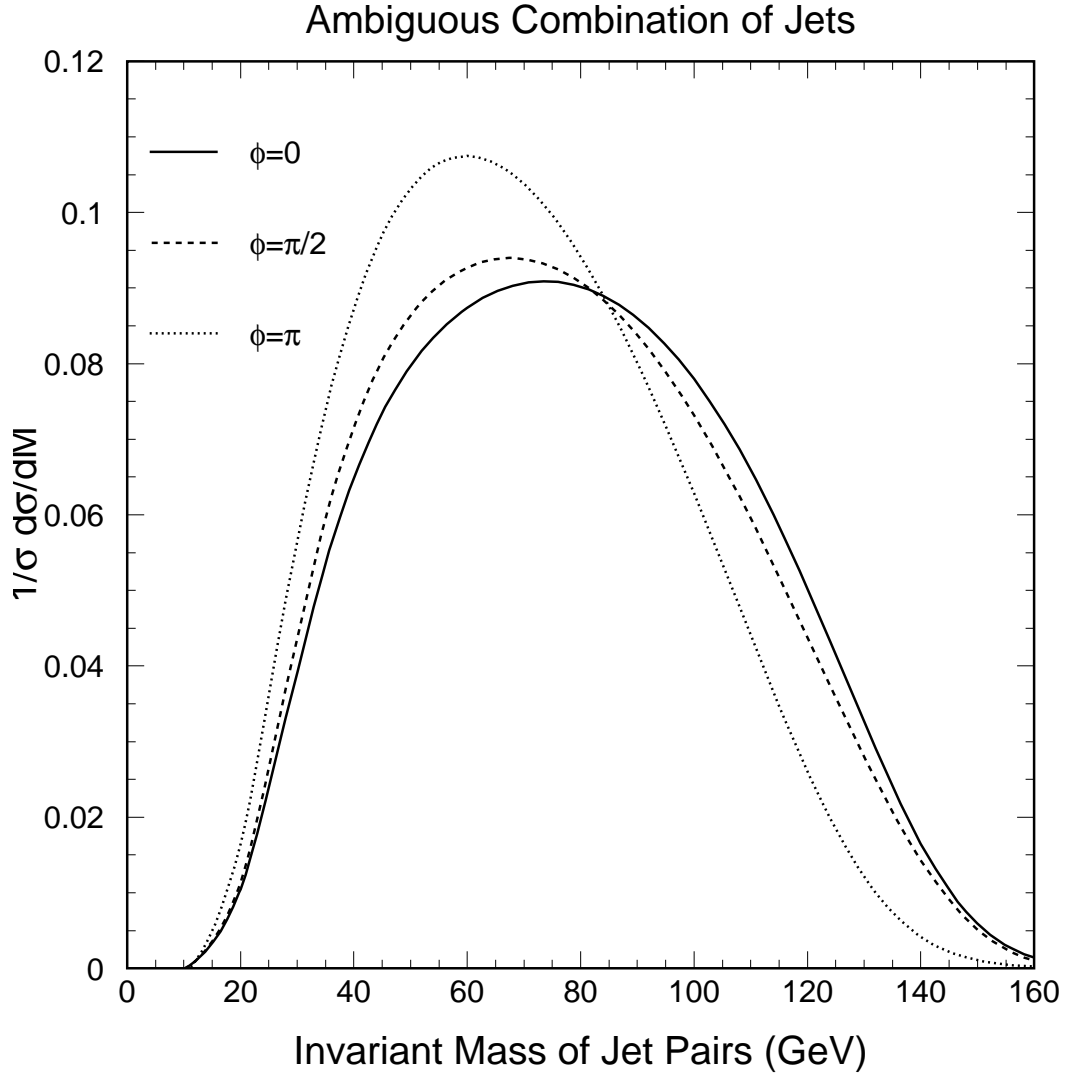


FIG. 2. Same as Fig. 1, except it is not assumed that the jets will always be paired correctly. Instead, the combination of jet pairs that minimizes the sum of the squared masses is used.

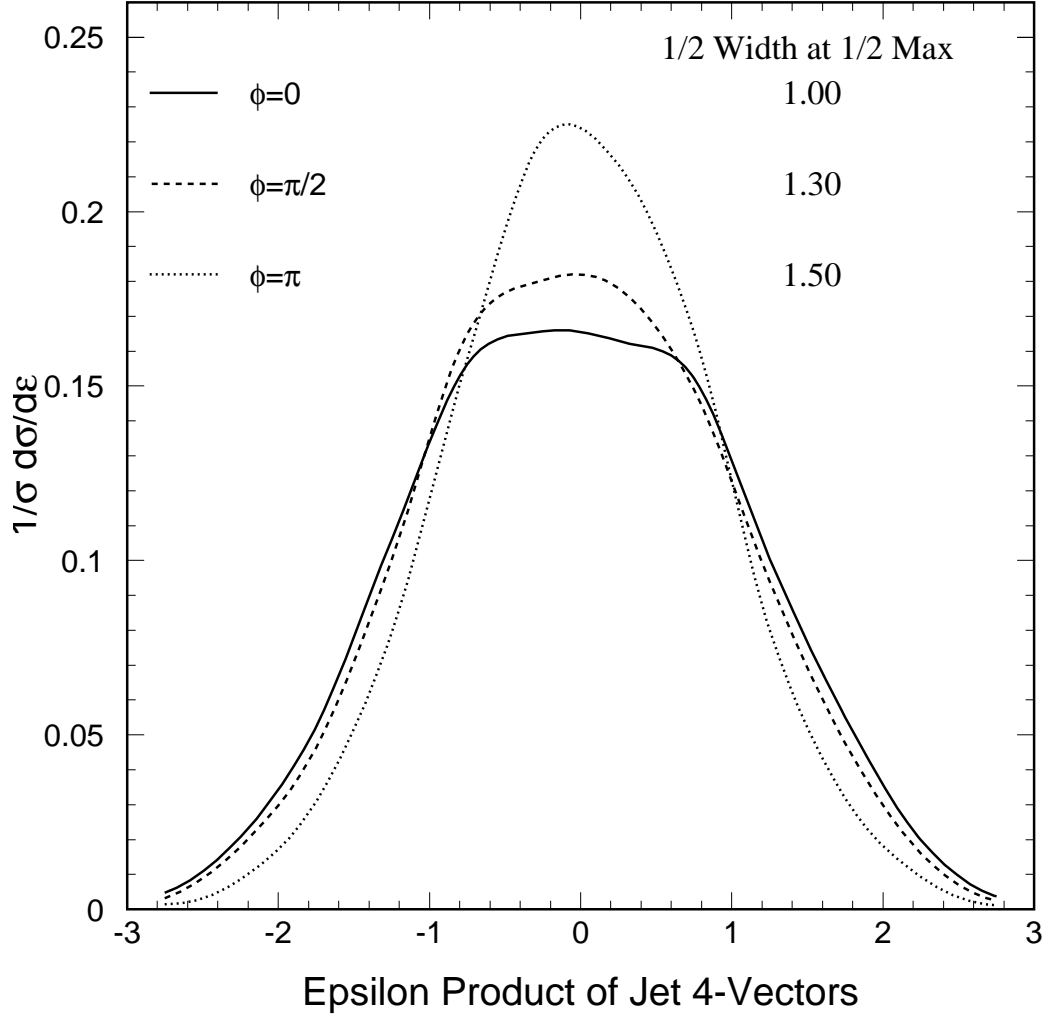


FIG. 3. A laboratory observable based on contracting the four momenta of the four jets with the Levi-Cevita tensor $\epsilon_{\mu\mu\sigma\rho}$. The distribution is normalized by the jet energies and is thus dimensionless. The different distributions and the half width at half maximum values for three different effective phases is shown.

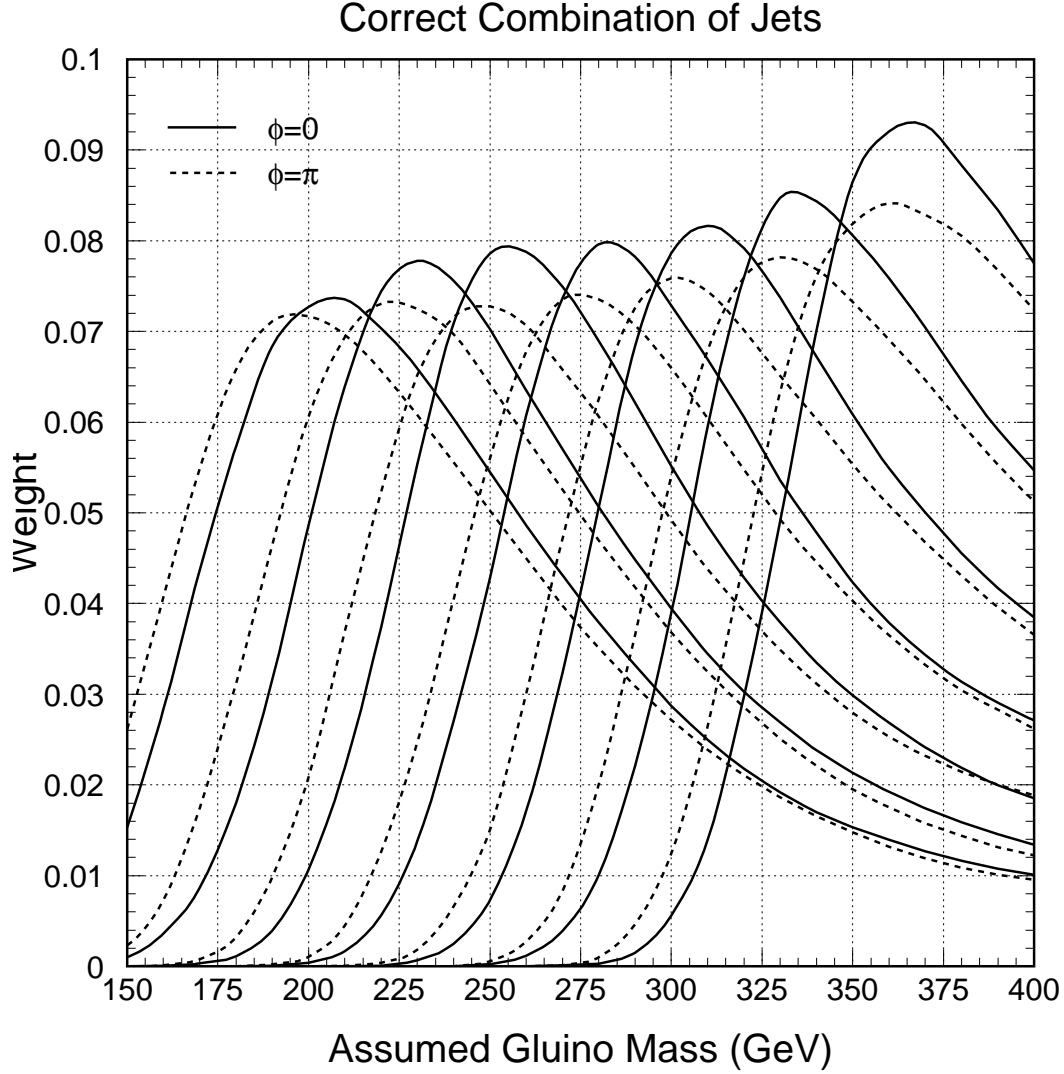


FIG. 4. Distribution of the probabilistic fits to the gluino mass for $m_{\tilde{g}} = 250 - 350$ GeV in 25 GeV steps. The peak of each distribution corresponds to the value of $m_{\tilde{g}}$ that best describes the kinematics of four jet plus \cancel{E}_T events. Also shown is the systematic shift in the distributions for different values of the effective phase. The correct combination of jet pairs is used to determine the gluino kinematics.

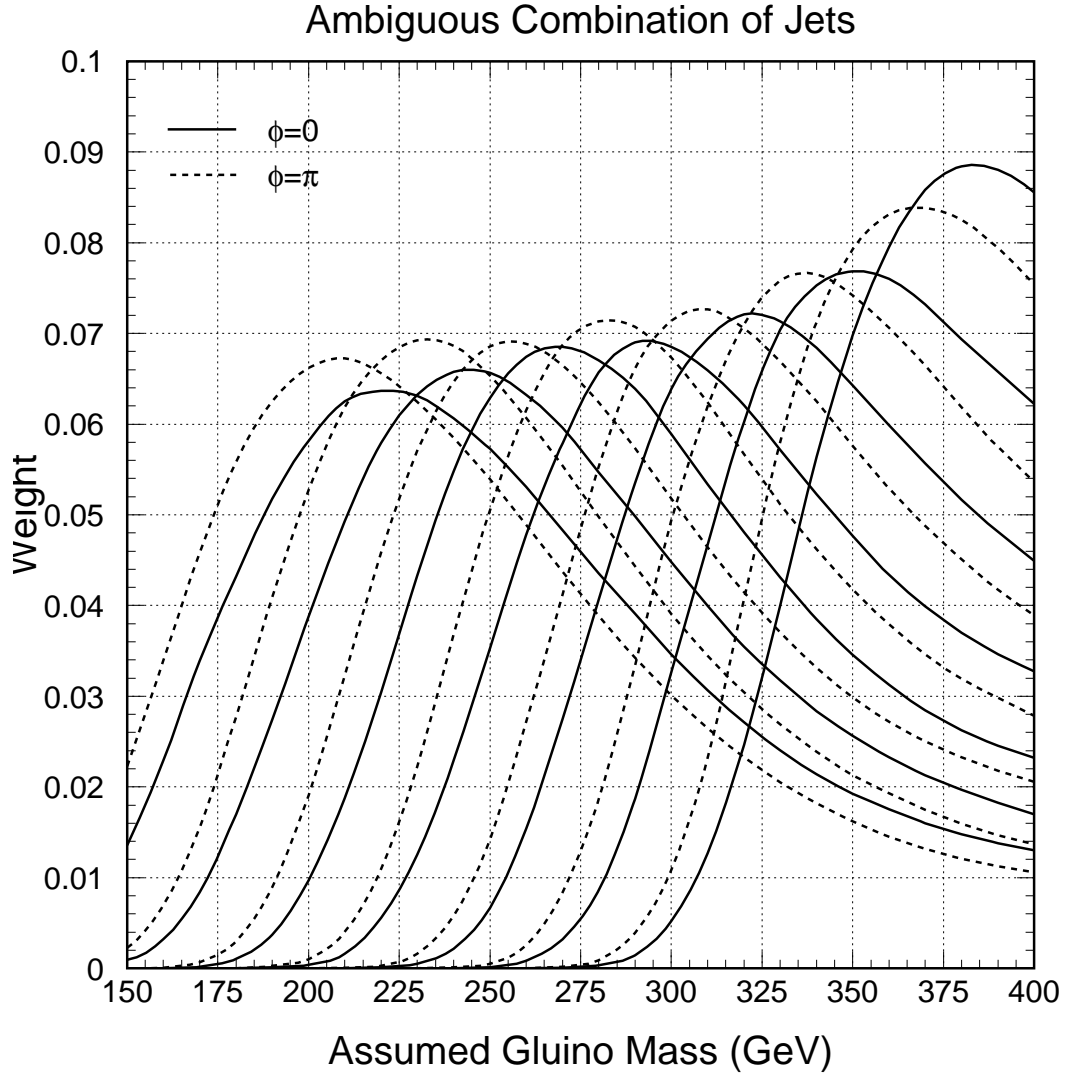


FIG. 5. Same as Fig. 5 but allowing for miscombination of the jet pairs. When the jets are mismatched, the gluino energy and momentum is shifted from its actual value.